EFFECT OF MINORITY ALLOYING ELEMENTS Zn AND Zr ON THE MECHANICAL PROPERTIES OF AMORPHOUS ALLOYS AlCuMg(Zn) AND AlCuMg(Zr) AND THEIR NANOCRYSTALLINE ANALOGUES

Vanya Dyakova[1*] and Sabina Cherneva[2]

[1] *Institute of Metal Science, Equipment and Technologies with Hydro- and Aerodynamics Centre "Acad. Angel Balevski", Bulgarian Academy of Sciences, 67, Shipchenski Prohod Blvd, 1574 Sofia, Bulgaria, e-mail: v_diakova@ims.bas.bg*

[2] *Institute of Mechanics, Bulgarian Academy of Sciences, Acad. G. Bonchev St., Bl. 4, 1113 Sofia, Bulgaria, e-mail: sabina_cherneva@yahoo.com*

Abstract. Effect of minority alloying elements Zn and Zr on the hardness and modulus of elasticity of amorphous alloys AlCuMg(Zn) and AlCuMg(Zr) and their nanocrystalline analogues was investigated by nanoindentation. It was found that the microalloying of $Al_{74}Cu_{16}Mg_{10}$ with less than 1 at.% Zr increases the modulus of elasticity of the amorphous and nanocrystalline alloys $(Al_{74}Cu_{16}Mg_{10})_{99.7}Zr_{0.3}$ compared to the amorphous and nanocrystalline alloys $Al_{74}Cu_{16}Mg_{10}$. The microalloying of $Al_{74}Cu_{16}Mg_{10}$ with 1 at.% Zn reduces the modulus of elasticity of both amorphous and nanocrystalline alloys $(Al_{74}Cu_{16}Mg_{10})_{99}Zn$ compared to their base alloys.

Keywords: aluminum alloys, amorphous, nanocrystalline, nanoindentation, hardness, modulus of elasticity.

1. INTRODUCTION

Metal glasses (amorphous metals) were discovered in 1960, but interest in them is still high [1]. Metallic glasses show unique physical and mechanical properties compared to their crystalline analogues [2–3]. They have an unusual combination of high yield strength and low modulus of Young, high limit of elastic strain and toughness [4]. But the lack of significant plastic deformation at room temperature is one of the reasons why their potential applications are limited [5–6].

---

[*] Corresponding author.

DOI: 10.7546/EngSci.LIX.22.02.04

Therefore, more and more attention is being paid to the study of the mechanical properties and deformation of metallic glass. In addition, the annealing of amorphous metals is one of the methods of obtaining materials with nanoscale microstructure.

One of the methods of studying the mechanical properties of amorphous and nanocrystalline materials is nanoidentation. The application of this method of research in quasi-brittle materials results in the accumulation of significant plastic deformation in localized areas, which is the basis for studying the mechanical response of the studied materials such as hardness and modulus of elasticity [7–9].

The aim of our study was to obtain data on the mechanical characteristics of the indentation hardness H_{IT} and the modulus of elasticity E_{IT} of the Al-Cu-Mg system amorphous alloys, with small amounts of Zn and Zr, and of their nanocrystalline analogues. We expect that our study will add new information on the influence of the chemical composition and microstructure of alloys on mechanical properties such as nanoindentation hardness and modulus of elasticity.

2. EXPERIMENTAL PART

2.1. Tested materials

Rapidly solidified and nanocrystalline Al-Cu-Mg alloys with minority amounts of Zn and Zr were studied. The alloy $Al_{74}Cu_{16}Mg_{10}$ was chosen in our work as a base alloy because it is known that metallic glasses are most easily obtained from alloys with eutectic composition [10]. One at.% Zn and 0.3 at.% Zr were added to the base alloy. Rapidly solidified alloys were obtained by the Chill Block Melt Spinning (CBMS) method in the form of ribbons from 42 to 120 µm thick. The synthesis of Al-Cu-Mg-Zn and Al-Cu-Mg-Zr alloys and the process of obtaining the ribbons are described in detail in our previous publications [11–12]. In order to transform the structure from amorphous to nanocrystalline, part of the ribbons were annealed at 300 °C for 1.5 h in argon environment in an electric arc furnace.

The tested specimens of rapidly solidified ribbons (r) and annealed specimens (a) are designated as follows:

(i) $Al_{74}Cu_{16}Mg_{10}$, or (3r), is the base alloy;
(ii) $Al_{74}Cu_{16}Mg_{10})_{99}Zn$, or (3r-1Zn), is the alloy with 1 at.% Zn;
(iii) $Al_{74}Cu_{16}Mg_{10})_{99,7}Zr_{0,3}$, or (3r-0.3Zr), is the alloy with 0.3 at.% Zr.

Further, down in this paper the rapidly solidified amorphous ribbons (r) will be called "amorphous alloys" and the annealed ribbons (a) will be called "nanocrystalline alloys".

The presence of the amorphous phase in all rapidly solidified alloys was studied and confirmed by X-ray Diffraction (XRD), Transmission Electron Microscopy (TEM) and Differential Scanning Calorimetry (DSC) [13]. The nanocrystalline structures of the alloys after annealing were analyzed by XRD again. The results from of the XRD analysis are given in Table 1.

The eutectic base alloy $Al_{74}Cu_{16}Mg_{10}$ is 98% amorphous. It was found that the addition of only 0.3 at.% zirconium to the base alloy is sufficient to achieve a 100% amorphous state in $(Al_{74}Cu_{16}Mg_{10})_{99.7}Zr_{0.3}$ under the same conditions of rapid solidification. And contrariwise, the addition of 1 at.% Zn reduces the amorphous part of the base alloy from 98% to 71% in $(Al_{74}Cu_{16}Mg_{10})_{99}Zn$. Previous studies with higher amounts of Zn have shown that with the increase of Zn amount to 2% and 3% the amorphous part of the ribbons decreases to 49% and 45%, respectively. The results were explained in terms of Free Volume Model (FVM) [14].

Table 1. Structural characteristics of $Al_{74}Cu_{16}Mg_{10}$, $(Al_{74}Cu_{16}Mg_{10})_{99}Zn$ and $(Al_{74}Cu_{16}Mg_{10})_{99.7}Zr_{0.3}$ amorphous and nanocrystalline alloys

Designations of alloys	Designations of specimens	Amorphous part, [%]	Crystalline part, [%]	Types of crystalline phases
$Al_{74}Cu_{16}Mg_{10}$-r	3r	98	2	Al; Al_2CuMg
$Al_{74}Cu_{16}Mg_{10}$-a	3ra	–	100	Al; Al_2CuMg
$(Al_{74}Cu_{16}Mg_{10})_{99}Zn$-r	3r-1Zn	71	29	Al; $Al_2(Cu,Zn)$; $Al_2(Cu,Zn)Mg$
$(Al_{74}Cu_{16}Mg_{10})_{99}Zn$-a	3r-1Zn-a	–	100	Al; (Cu,Zn) Al_2; $Al_2(Cu,Zn)Mg$
$(Al_{74}Cu_{16}Mg_{10})_{99.7}Zr_{0.3}$-r	3r-0.3Zr	100	–	–
$(Al_{74}Cu_{16}Mg_{10})_{99.7}Zr_{0.3}$-a	3r-0.3Zr-a	–	100	Al; Al_2CuMg; $CuAl_2$; Al_3Zr_4

2.2. Nanoindentation as test method

Nanoindentation is a new type of mechanical testing. The tested material is loaded gradually. High-resolution devices perform continuous control of the loads and displacements of the indenter from its pressing into the material until it is pulled out of it. The mechanical characteristics of the material are obtained from the load–displacement curve. They are determined by the indenter footprint smaller than 1 micron and only a few nanometers deep.

Fig. 1. Nanoindentor G200

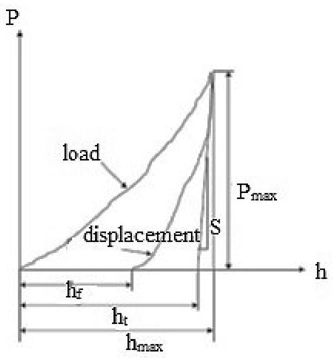

Fig. 2. Load–displacement curve obtained by nanoindentation

In our studies, the measurements were made with Nano Indenter G200 (KLA Corporation, California, USA) Fig. 1, equipped with a three-walled diamond pyramid of Berkovich with 20 nm rounding at the top in accordance with ISO 14577. Between 15 and 18 indentations were made on each sample at 100 mN maximum load.

When the indenter penetrates the material, processes of elastic and plastic deformation take place and an imprint with contact depth h_c and radius a is obtained. When the indenter is pulled out, only the elastic part of the displacements is restored, which allows for highly effective separation of the elastic properties of the material from the plastic ones.

The curves obtained during a complete cycle of loading and unloading of the indenter are shown schematically in Fig. 2.

The values on the basis of which the mechanical characteristics of hardness H and modulus of elasticity E are determined are as follows: maximum load $P_{\max}$, maximum penetration depth $h_{\max}$, residual depth after unloading h_f, and slope of the unloading curve $S\,(S = dP/dh)$. The parameter S has a dimension of force per unit distance and is known as elastic contact stiffness.

The main relationships that determine H and E are:

$$H = \frac{P}{A}, \tag{1}$$

where A is the contact area at this load,

$$E_r = \frac{\sqrt{\pi}}{2\beta}\frac{S}{\sqrt{A}}, \tag{2}$$

where E_r is the reduced elastic modulus and β is a constant that depends on the geometry of the indenter.

The elastic modulus E of the test material is calculated from the reduced elastic modulus E_r:

$$\frac{1}{E_r} = \frac{1-\nu^2}{E} + \frac{1-\nu_i^2}{E_i}, \tag{3}$$

where ν is Poisson's ratio of the tested material, and E_i and ν_i are the elastic modulus and Poisson's ratio of the material from which the indenter is made, respectively.

Equations (1) and (2) show that in order to calculate the hardness and elastic moduli, there must be accurately measured elastic contact stiffness S and contact area A. The most widely used method of determining the contact area was developed by Oliver & Pharr.

Oliver & Pharr's method begins with an approximation of that part of the load-displacement curve that corresponds to the unloading by the power relation:

$$P = B(h - h_f)^m, \tag{4}$$

where B and m are empirically determined parameters of the approximation, and h_f is the final displacement of the indenter after unloading is completed. The contact stiffness S is determined by analytical differentiation of equation (4) and calculation of the result at maximum penetration depth $h = h_{\max}$, i.e.:

$$S = \left(\frac{dP}{dh}\right)_{(h_{\max},\ P_{\max})} = Bm\left(h_{\max} - h_f\right)^{m-1}, \tag{5}$$

The next step is to determine the contact depth h_c:

$$h_c = h - \varepsilon\frac{P}{S}, \tag{6}$$

where ε is a constant that depends on the geometry of the indenter.

The last step in the analysis is to calculate the contact area using:

$$A = \pi \left(h_{\max} - 0.75 \frac{P_{\max}}{S} \right)^2 tan^2(\varphi), \tag{7}$$

where φ is the angle of the indenter.

Once A and S are determined, the stiffness and elastic moduli are determined by equations (1) and (3).

3. RESULTS AND DISCUSSION

As a result of the nanoindentation experiment, the load–displacement curves for each of the studied amorphous and nanocrystalline alloys were obtained (Figs 3–8) and the indentation hardness H_{IT} and modulus E_{IT} were calculated using the Oliver & Pharr approximation method.

Calculated indentation hardness H_{IT} [GPa] and modulus E_{IT} [GPa] of the tested alloys are presented in Figs 9–10 and Table 2.

The following indicators are introduced for comparison between the obtained results for the studied amorphous and nanocrystalline alloys:

$A_H = \dfrac{Hr}{Ha}$ indicates how many times the hardness of each amorphous alloy is bigger (> 1) or smaller (< 1) than the hardness of its nanocrystalline analogue;

$B_H = \dfrac{Hr}{Hrb}$ indicates how many times the hardness of the amorphous alloy is bigger (> 1) or smaller (< 1) than the hardness of its base amorphous analogue;

$C_H = \dfrac{Ha}{Hab}$ indicates how many times the hardness of the nanocrystalline alloy is bigger (> 1) or smaller (< 1) than the hardness of its base nanocrystalline analogue;

$A_E = \dfrac{Er}{Ea}$ indicates how many times the modulus of elasticity of the amorphous alloy is bigger (> 1) or smaller (< 1) than the modulus of elasticity of its nanocrystalline analogue;

$B_E = \dfrac{Er}{Erb}$ indicates how many times the modulus of elasticity of the amorphous alloy is bigger (> 1) or smaller (< 1) than the modulus of elasticity of its base amorphous analogue;

$C_E = \dfrac{Ea}{Eab}$ indicates how many times the modulus of elasticity of the

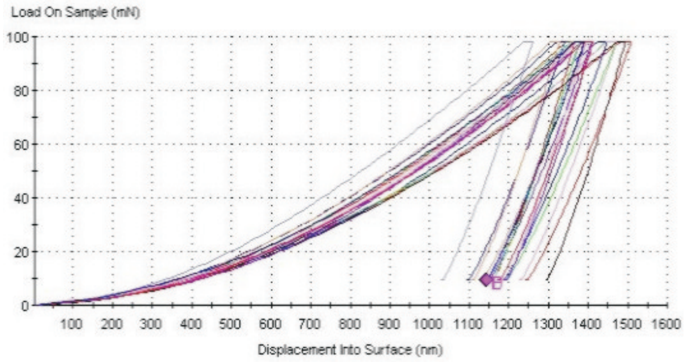

Fig. 3. Experimental load–displacemen curve for a sample 3r

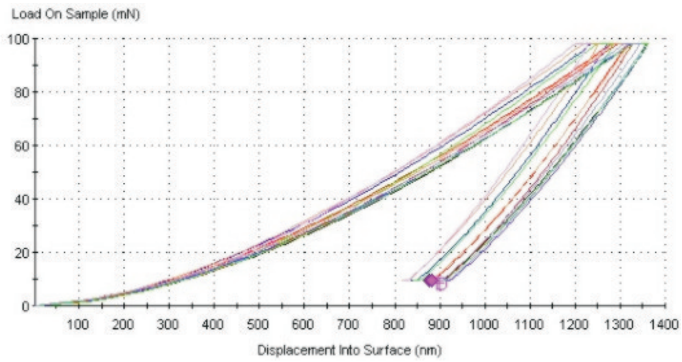

Fig. 4. Experimental load–displacement curve for a sample 3ra

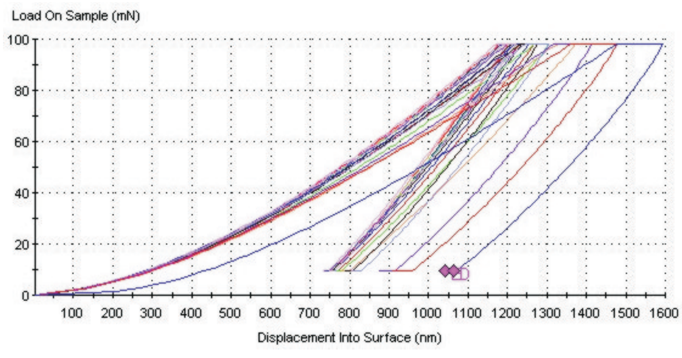

Fig. 5. Experimental load–displacement curve for a sample 3r-1Zn

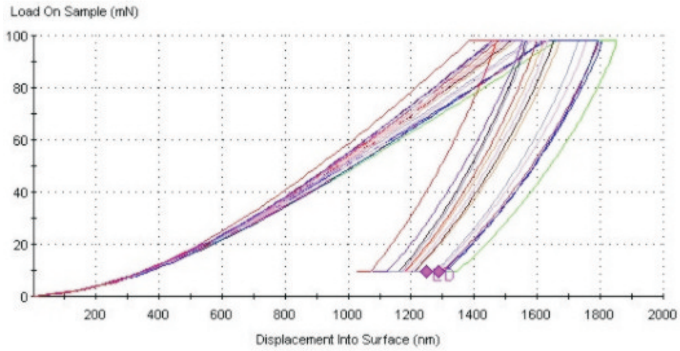

Fig. 6. Experimental load–displacement curve for a sample 3r-1Zn-a

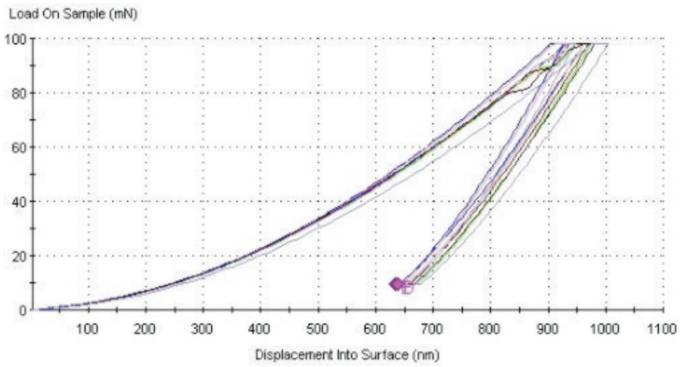

Fig.7. Experimental load–displacement curve for a sample 3r-0.3Zr

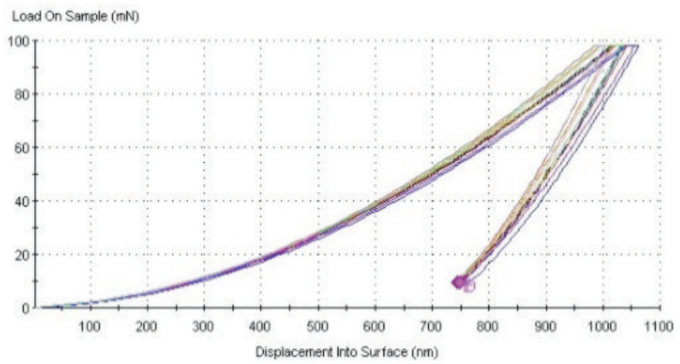

Fig. 8. Experimental load–displacement curve for a sample 3r-0.3Zr-a

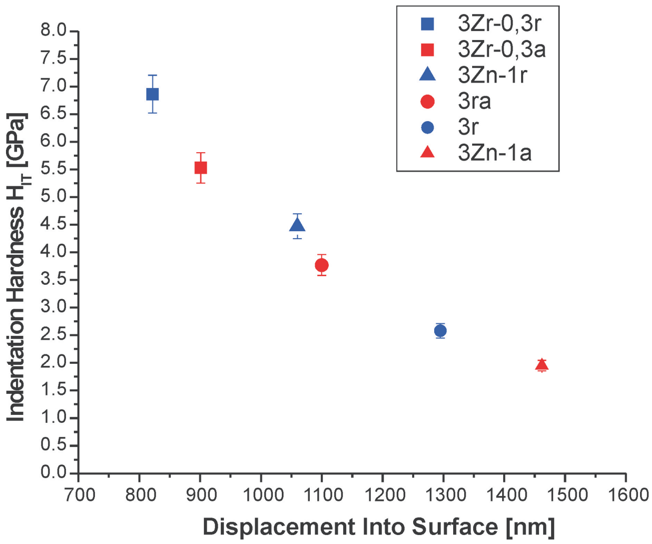

Fig. 9. Indentation hardness H_{IT} of the studied specimens

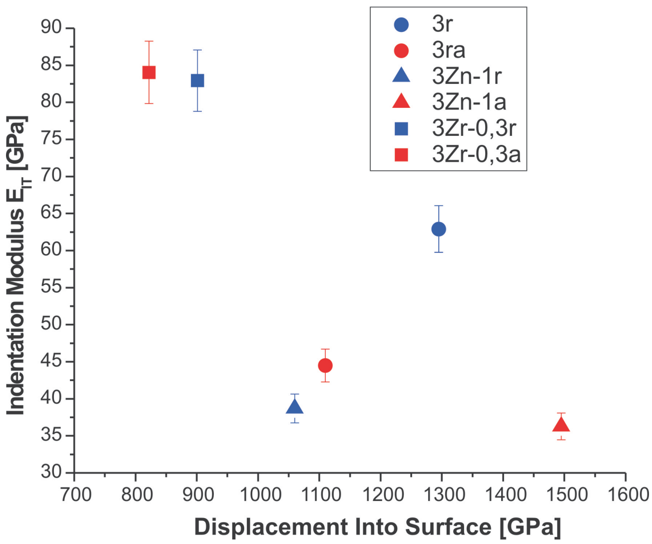

Fig. 10. Indentation modulus E_{IT} of the studied specimens

nanocrystalline alloy is bigger (> 1) or smaller (< 1) than the modulus of elasticity of its base nanocrystalline analogue.

The results of the tested alloys show that:

- The amorphous alloy with 0.3 at.% Zr $(Al_{74}Cu_{16}Mg_{10})_{99.7}Zr_{0.3}$-r has the

Table 2. Results of the nanoindentation test

Designations of alloys	Hardness H_{IT} [GPa]	A_H	B_H	C_H	Modulus E_{IT} [GPa]	A_E	B_E	C_E
3r	2.58 ± 0.25	0.68	–	–	62.91 ± 7.76	1.41	–	–
3ra	3.77 ± 0.28		–	–	44.49 ± 3.06		–	–
3r-1Zn	4.47 ± 0.84	2.29	1.73	–	38.70 ± 4.30	1.07	0.62	–
3r-1Zn-a	1.95 ± 0.28		–	0.52	36.23 ± 4.23		–	0.81
3r-0.3Zr	6.86 ± 0.26	1.24	2.66	–	82.93 ± 6.61	0.99	1.32	–
3r-0.3Zr-a	5.53 ± 0.15		–	1.46	84.05 ± 7.07		–	1.89

highest indentation hardness, followed by the nanocrystalline alloy with the same composition;

- The nanocrystalline alloy with 1 at.% Zn $(Al_{74}Cu_{16}Mg_{10})_{99}Zn$ has the lowest indentation hardness;
- The amorphous alloy $(Al_{74}Cu_{16}Mg_{10})_{99.7}Zr_{0.3}$-r has the highest indentation modulus of elasticity of the amorphous alloys, but the modulus of elasticity of the nanocrystalline alloy $(Al_{74}Cu_{16}Mg_{10})_{99.7}Zr_{0.3}$-a is 1.13% higher than that of the amorphous alloy with the same composition
- The nanocrystalline alloy $(Al_{74}Cu_{16}Mg_{10})_{99}Zn$-a has the lowest indentation modulus of elasticity of the tested alloys. The modulus of elasticity of the amorphous alloy $(Al_{74}Cu_{16}Mg_{10})_{99}Zn$-r is higher than that of the nanocrystalline alloy $(Al_{74}Cu_{16}Mg_{10})_{99}Zn$-a by 5.17%.
- The modulus of elasticity of the basic amorphous alloy $Al_{74}Cu_{16}Mg_{10}$ is about 30% higher than of its nanocrystalline analogue.

The results of H_{IT} and E_{IT} obtained for the amorphous alloys $(Al_{74}Cu_{16}Mg_{10})_{99}Zn$ and $(Al_{74}Cu_{16}Mg_{10})_{99.7}Zr_{0.3}$, except the result of the hardness for amorphous $(Al_{74}Cu_{16}Mg_{10})_{99}Zn$ alloy, can be explained by the efficiency of the cluster packaging and the degree of amorphousness of alloys after the introduction of Zn and Zr atoms in AlCuMg system. The atomic radius of Zn – 134 pm is slightly smaller than the atomic radius of Al – 143 pm. Addition of Zn atoms in $Al_{74}Cu_{16}Mg_{10}$ alloy increases the free volume in the atomic clusters and reduces the packaging efficiency. The introduction of Zr atoms with a radius of 160 pm into the $Al_{74}Cu_{16}Mg_{10}$ alloy reduces the free volume in the clusters and increases the efficiency of the cluster package in the $(Al_{74}Cu_{16}Mg_{10})_{99.7}Zr_{0.3}$ alloy. Probably this is the main reason for the increasing the hardness and modulus of elasticity of the alloy containing Zr compared to base $Al_{74}Cu_{16}Mg_{10}$ alloy.

CONCLUSIONS

The microalloying of $Al_{74}Cu_{16}Mg_{10}$ with less than 1 at.% Zr increases the degree of amorphousness of the rapidly solidified alloy $(Al_{74}Cu_{16}Mg_{10})_{99.7}Zr_{0.3}$ to 100%; increases the hardness of the amorphous and nanocrystalline alloys $(Al_{74}Cu_{16}Mg_{10})_{99.7}Zr_{0.3}$ 2.7 and 1.5 times and the modulus of elasticity of these alloys 1.3 and 1.9 times, respectively, compared to the base amorphous and nanocrystalline alloys $Al_{74}Cu_{16}Mg_{10.}$

The microalloying of $Al_{74}Cu1_{6}Mg_{10}$ with 1 at.% Zn reduces the degree of amorphousness of the rapidly solidified alloy $(Al_{74}Cu_{16}Mg_{10})_{99}Zn$ to 71%; increases the hardness of the amorphous alloy $(Al_{74}Cu_{16}Mg_{10})_{99}Zn$ 1.73 times and reduces the hardness of the nanocrystalline alloy $(Al_{74}Cu_{16}Mg_{10})_{99}Zn$-a 0.52 times compared to the base amorphous and nanocrystalline alloys $Al_{74}Cu_{16}Mg_{10}$; reduces the modulus of elasticity of the amorphous and nanocrystalline alloys $(Al_{74}Cu_{16}Mg_{10})_{99}Zn$ 0.62 and 0.81 times, respectively, compared to the base amorphous and nanocrystalline alloys $Al_{74}Cu_{16}Mg_{10}$.

ACKNOWLEDGEMENTS

The research in this publication is funded under the project "Study of the rheological and corrosion behaviour of amorphous and nanocrystalline aluminium-based alloys," Contract with BNCF No KP-06-H37/13 from 06 December 2019.

REFERENCES

[1] W. Klementjun, R. H. Willens, and Pol Duwez, *Nature* (1960) **187** 869–870, doi: 10.1038/187869b0.

[2] W. Zhou, X. Lin, and J. F. Li, Effects of Ag Addition on Crystallization, Microstructure and Mechanical Properties of Zr-Cu-Ni-Al-Ag Bulk Metallic Glasses, *Journal of Alloys and Compounds* (2013) **552** 102–106.

[3] G. R. Garrett, M. D. Demetriou, J. Chenand, and W. L. Johnson, Effect of Microalloying on the Toughness of Metallic Glasses, *Applied Physics Letters* (2012) **101** (24) Article ID 241913 6.

[4] H. Gleiter, *Metallurgical and Materials Transactions* A, 40A (2009) 1499–1509.

[5] W. L. Johnson, Bulk Glass-Forming Metallic Alloys: Science and Technology, *Materials Research Society Bulletin* (1999) **24** (10) 42–56.

[6] J. Eckert, J. Das, S. Pauly, and C. Duhamel, Mechanical Properties of Bulk Metallic Glasses and Composites, *Journal of Materials Research* (2007) **22** (2) 285–301.

[7] N. Li, L. Liu, K. C. Chan, Q. Chenand, and J. Pan, Deformation Behavior and Indentation Size Effect of Au49Ag5.5Pd2.3Cu26.9Si16.3 Bulk Metallic Glass at Elevated Temperatures, *Intermetallics* (2009) **17** (4) 227–230.

[8] C. A. Schuh and T. G. Nieh, A Nanoindentation Study of Serrated Flow in Bulk Metallic Glasses, *Acta Materialia* (2003) **51** (1) 87–99.

[9] B. G. Yoo, K. W. Lee, and J. I. Jang, Instrumented Indentation of a Pd-based Bulk Metallic Glass: Constant Loading-Rate Test vs Constant Strain-Rate Test, *Journal of Alloys and Compounds* (2009) **483** (1–2) 136–138.

[10] Inoue Akihisa, Amorphous, Nanoquasicrystalline and Nanocrystalline Alloys in Al-Based Systems, *Progress in Materials Science* (1998) **43** 365–520, DOI: 10.1016/S0079-6425(98)00005-X.

[11] V. Dyakova, G. Stefanov, D. Kovacheva, and Y. Murdjeva, Rapidly Solidified Al-Cu-Mg Amorphous and Nanocrystalline Alloys, *International Journal "DNT Days"* (2020) **VIII** (3) 154–159.

[12] I. Penkov, N. Marinkov, G. Stefanov, V. Dyakova, D. Kichukova, and Y. Murdzjeva, Glass Forming Ability and Crystallization Behaviour of Amorphous and Nanosized Rapidly Solidified (Al75Cu17Mg8)100-xZnx Aloys, *Machines. Technologies. Materials* (2020) **XIV** (8) 366–369, ISSN: 1313-0226, e-ISSN: 1314-507X.

[13] V. Dyakova, G. Stefanov, D. Kovacheva, Y. Mourdjeva, N. Marinkov, I. Penkov, and J. Georgiev, Influence of Zr and Zn as Minority Alloying Elements on Glass Forming Ability and Crystallization Behaviour of Rapidly Solidified AlCuMg Ribbons, in: API Conference proceedings, 2021, e-ISSN: 1551-7616 (in print).

[14] V. Dyakova, G. Stefanov, I. Penkov, D. Kovacheva, N. Marinkov, Y. Mourdjeva, and S. Gyurov, Influence of Zn on Glass Forming Ability and Crystallization Behaviour of Rapidly Solidified Al-Cu-Mg (Zn) Alloys, *Journal of Chemical Technology and Metallurgy* (2022) **57** (3).

Received March 18, 2022